BEST AVAILABLE IMAGES

Defective images within this document are accurate representations of the original documents submitted by the applicant.

Defects in the images may include (but are not limited to):

- BLACK BORDERS
- TEXT CUT OFF AT TOP, BOTTOM OR SIDES
- FADED TEXT
- ILLEGIBLE TEXT
- SKEWED/SLANTED IMAGES
- COLORED PHOTOS
- BLACK OR VERY BLACK AND WHITE DARK PHOTOS
- GRAY SCALE DOCUMENTS

IMAGES ARE BEST AVAILABLE COPY.

As rescanning documents *will not* correct images, please do not report the images to the Image Problem Mailbox.

1. Nussbaum, O., Broder, C.C. & Berger, E.A. Fusogenic mechanisms of enveloped-virus glycoproteins analyzed by a novel recombinant vaccinia virus-based assay quantitating cell fusion-dependent reporter gene activation. *J. Virol.* **68**, 5411–5422 (1994).
2. Lineberger, J.E., Danzeisen, R., Hazuda, D.J., Simon, A.J. & Miller, M.D. Altering expression levels of human immunodeficiency virus type 1 gp120-gp41 affects efficiency but not kinetics of cell–cell fusion. *J. Virol.* **76**, 3522–3533 (2002).
3. Nguyen, D.H. & Hildreth, J.E. Evidence for budding of human immunodeficiency virus type 1 selectively from glycolipid-enriched membrane lipid rafts. *J. Virol.* **74**, 3264–3272 (2000).
4. Aloia, R.C., Tian, H. & Jensen, F.C. Lipid composition and fluidity of the human immunodeficiency virus envelope and host cell plasma membranes. *Proc. Natl. Acad. Sci. USA* **90**, 5181–5185 (1993).
5. Tremblay, M.J., Fortin, J.F. & Cantin, R. The acquisition of host-encoded proteins by nascent HIV-1. *Immunol. Today* **19**, 346–351 (1998).
6. Lowy, R.J., Sarkar, D.P., Chen, Y. & Blumenthal, R. Observation of single influenza virus-cell fusion and measurement by fluorescence video microscopy. *Proc. Natl. Acad. Sci. USA* **87**, 1850–1854 (1990).
7. Chen, Y.D. & Blumenthal, R. On the use of self-quenching fluorophores in the study of membrane fusion kinetics. The effect of slow probe redistribution. *Biophys. Chem.* **34**, 283–292 (1989).
8. Raviv, Y., Viard, M., Bess, J., Jr. & Blumenthal, R. Quantitative measurement of fusion of HIV-1 and SIV with cultured cells using photosensitized labeling. *Virology* **293**, 243–251 (2002).
9. Bridger, G.J. *et al.* Synthesis and structure–activity relationships of phenylenebis(methylene)-linked bis-tetraazamacrocycles that inhibit HIV replication. Effects of macrocyclic ring size and substituents on the aromatic linker. *J. Med. Chem.* **38**, 366–378 (1995).
10. Schols, D. *et al.* Inhibition of T-tropic HIV strains by selective antagonization of the chemokine receptor CXCR4. *J. Exp. Med.* **186**, 1383–1388 (1997).
11. Marechal, V., Clavel, F., Heard, J.M. & Schwartz, O. Cytosolic Gag p24 as an index of productive entry of human immunodeficiency virus type 1. *J. Virol.* **72**, 2208–2212 (1998).
12. Schaeffer, E., Geleziunas, R. & Greene, W.C. Human immunodeficiency virus type 1 Nef functions at the level of virus entry by enhancing cytoplasmic delivery of virions. *J. Virol.* **75**, 2993–3000 (2001).
13. Baba, M. *et al.* A small-molecule, nonpeptide CCR5 antagonist with highly potent and selective anti-HIV-1 activity. *Proc. Natl. Acad. Sci. USA* **96**, 5698–5703 (1999).
14. Eckstein, D.A. *et al.* HIV-1 actively replicates in naive CD4(+) T cells residing within human lymphoid tissues. *Immunity* **15**, 671–682 (2001).
15. de Noronha, C.M. *et al.* Dynamic disruptions in nuclear envelope architecture and integrity induced by HIV-1 Vpr. *Science* **294**, 1105–1108 (2001).
16. Zlokarnik, G. *et al.* Quantitation of transcription and clonal selection of single living cells with β-lactamase as reporter. *Science* **279**, 84–88 (1998).

Arrayed adenoviral expression libraries for functional screening

Frits Michiels[1], Helmuth van Es[1]*, Luc van Rompaey[2], Pascal Merchiers[2], Bart Francken[2], Karen Pittois[2], Jan van der Schueren[2], Reginald Brys[2], Johan Vandersmissen[2], Filip Beirinckx[2], Sofie Herman[2], Kristina Dokic[1], Hugo Klaassen[2], Evi Narinx[2], Annick Hagers[2], Wendy Laenen[2], Ivo Piest[1], Heidi Pavliska[1], Yvonne Rombout[1], Ellen Langemeijer[1], Libin Ma[1], Christel Schipper[1], Marc De Raeymaeker[2], Stephane Schweicher[2], Mia Jans[2], Kris van Beeck[2], Ing-Ren Tsang[2], Onno van de Stolpe[1,2], and Peter Tomme[2]

Published online: 30 September 2002, doi:10.1038/nbt746

With the publication of the sequence of the human genome, we are challenged to identify the functions of an estimated 70,000 human genes[1,2] and the much larger number of proteins encoded by these genes. Of particular interest is the identification of gene products that play a role in human disease pathways, as these proteins include potential new targets that may lead to improved therapeutic strategies. This requires the direct measurement of gene function on a genomic scale in cell-based, functional assays. We have constructed and validated an individually arrayed, replication-defective adenoviral library harboring human cDNAs, termed PhenoSelect library. The adenoviral vector guarantees efficient transduction of diverse cell types, including primary cells. The arrayed format allows screening of this library in a variety of cellular assays in search for gene(s) that, by overexpression, induce a particular disease-related phenotype. The great majority of phenotypic assays, including morphological assays, can be screened with arrayed libraries. In contrast, pooled-library approaches often rely on phenotype-based isolation or selection of single cells by employing a flow cytometer or screening for cell survival. An arrayed placental PhenoSelect library was screened in cellular assays aimed at identifying regulators of osteogenesis, metastasis, and angiogenesis. This resulted in the identification of known regulators, as well as novel sequences that encode proteins hitherto not known to play a role in these pathways. These results establish the value of the PhenoSelect platform, in combination with cellular screens, for gene function discovery.

We have generated an individually arrayed, adenoviral cDNA library from a 12-week-old human placenta, a tissue known to express a diverse set of genes. The adenoviral vector system is based on the adenovirus serotype 5 genome (Ad5), from which the E1 and E2A regions have been deleted. These regions are included in the

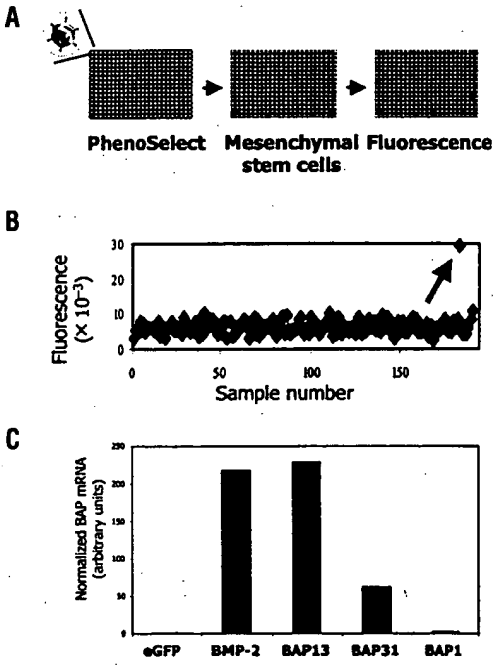

Figure 1. Induction of osteoblast formation. (A) To identify factors that induce osteoblast differentiation, mesenchymal stem cells were seeded in 384-well plates and infected in duplicate with individual adenoviruses from the placental cDNA library. Alkaline phosphatase (AP) activity was determined using 4-methylumbelliferyl heptaphosphate (MUP) six days after infection. (B) Graphic representation of a 384-well plate showing average AP activity. Arrow indicates a positive result. (C) Primary human MSC were infected with BMP-2 (positive) or enhanced green fluorescent protein (eGFP; negative) control viruses and the hit viruses BAP1, BAP13, and BAP31. Total RNA was isolated seven days after infection and used in Real-time PCR analyses to detect bone-specific alkaline phosphatase mRNA. Data were normalized for GAPDH expression levels.

[1]*Galapagos Genomics, Archimedesweg 4, 2333 CN Leiden, The Netherlands.*
[2]*Galapagos Genomics, Generaal de Wittelaan L11 A3, 2800 Mechelen, Belgium.*
**Corresponding author (es@galapagos.be).*

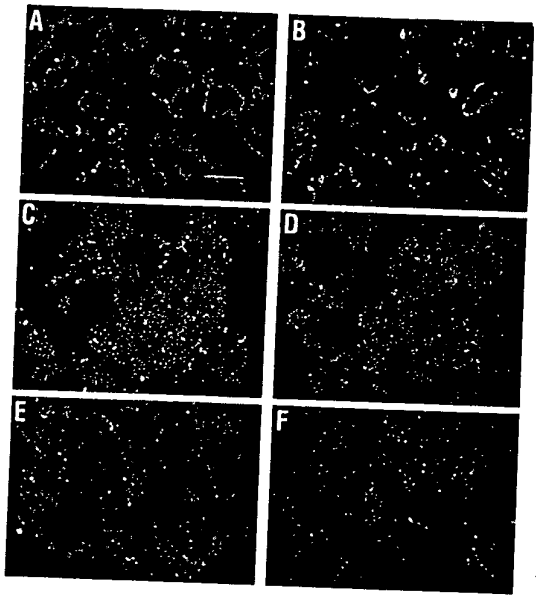

Figure 2. Loss of epithelial phenotype. Epithelial MDCK cells were infected with the adenoviral library in 96-well plates at an average MOI of 2,500, and cells were stained after 48 h with calcein-AM. Wells were visually inspected, and images of wells were recorded. The bar indicates 250 μm. (A) No virus added; (B) cells transduced with empty virus; (C) cells infected with viruses transducing oncogenic (L61) Ras; (D–F) cells transduced with placental library hits MET12 (endothelin receptor B), MET21 (wt-Ha-Ras), and MET25 (p57Kip2), respectively. Cells remain epithelial in (A) and (B), whereas in (C–F), they have scattered.

PER.C6/E2A packaging cell line[3], without any sequence overlap with the adenoviral vector. These features allow the production of functional, but replication-defective, adenoviral vectors, thus eliminating viral replication and its effects in the target cells after transduction.

The primary placenta cDNA library was directionally cloned into an adenoviral adapter plasmid[4]. To generate a nonbiased cDNA library, we grew individual bacterial clones in 96-well plates, and then individually co-transfected isolated adapter DNA with a helper plasmid into PER.C6/E2A packaging cells, resulting in live, replication-defective adenoviruses. A cytomegalovirus (CMV) promoter controls the expression of the cDNAs from the adenovirus. Protein expression is detected as early as 6 h after transduction, and can last for up to four weeks, depending on the individual cDNA and the cell type examined (data not shown). The expression level of the transgenes correlates with the multiplicity of infection (MOI) that is used for transduction (refer to Fig. 3B). Furthermore, cells are homogeneously transduced, even at low MOIs (data not shown).

Viral production was carried out in 96-well plates using a semiautomated, high-throughput system (see Experimental Protocol), allowing the generation of >12,000 viruses per week. The efficiency of virus generation, based on the number of wells that contained viruses after propagation, was ~85%. Sequence analyses revealed that 96% of the adenoviruses contained inserts. The average insert size was 1.9 kilobases, while the largest adenoviral insert identified was 8 kilobases. Of the known, annotated sequences, 29% encoded full-length proteins. The placenta PhenoSelect library contains >120,000 adenoviruses and shows little redundancy (data not shown). The average titer of the crude lysates was 2.5×10^9 viral particles/ml as determined on ~1,200 viruses of the library by real-time PCR[5].

The main advantage of adenovirus is its broad tropism. A list of primary cells and cell lines that can be infected with adenoviruses is available in Supplementary Table 1 online. Furthermore, coinfection with the human coxsackievirus and adenovirus receptor (hCAR)[6] often increases transduction efficiencies (data not shown; see also Fig. 1 and Experimental Protocol).

An amplified, pooled expression library normally consists of $>10^8$ clones to ensure the original complexity of the library. Such high numbers are not required for an arrayed library because of the absence of bias, with all steps after transformation in *Escherichia coli* being carried out individually. The current size of the arrayed placental library (120,000 viruses) is not sufficient to encompass all rare transcripts or splice variants. Therefore, we are currently expanding our collection by adding cDNA libraries (e.g., fetal liver and brain) and by generating a defined library containing known transcripts of small-molecule tractable proteins (druggable targets), including G protein–coupled receptors (GPCRs), kinases, and phosphatases. By using high-quality and rigorous bioinformatics to generate an arrayed, defined adenoviral library, one can increase its transcriptome coverage. This will at the same time decrease the high costs associated with the building and screening of an arrayed library large enough to to cover the human transcriptome.

To prove the feasibility of this screening platform, we used 13,000 viruses of the placental library in three independent assays aimed at identifying novel regulators in diverse disease-related pathways. All assays were miniaturized and validated with viruses transducing known regulators of these pathways. The primary hit rate of ~0.2% illustrates the minimally disruptive nature of E1/E2A-deleted adenoviruses.

To isolate factors that induce osteoblast differentiation from precursor cells, we transduced primary human mesenchymal stem cells (MSC) with adenoviruses using bone morphogenetic protein-2 (BMP-2) as a positive control. The induction of alkaline phosphatase (AP) activity was used as a well-established marker for osteoblast differentiation[7]. We identified a total of seven hits that induced alkaline phosphatase activity in the infected MSC, which all scored above the average + 3 s.d. (Fig. 1B). Three of these hits induced upregulation of alkaline phosphatase activity through a secreted protein as determined by transfer of supernatant from infected cells to MSC (data not shown). Real-time PCR indicated that one of these, hit BAP1, induced placental alkaline phosphatase or intestinal alkaline phosphatase (data not shown), while BAP13 and BAP31 induced bone-specific alkaline phosphatase (Fig. 1C). The latter were found to encode BMP-4 and BMP-7, respectively, two known inducers of osteoblast differentiation[8], thereby validating the assay and the screening procedure.

One of the four hits that functioned only by direct infection of MSC (BAP0) encoded FosB, an inducer of bone formation in transgenic mice[9]. BAP25 (GenBank NM_003206), BAP64 (M31222 lacking the DNA-binding domain), and BAP72 (M62324) encoded transcription factors and are being analyzed for the induction of other bone-specific markers in MSC.

The epithelial Madin Darbey canine kidney (MDCK-2) cell line[10] was used to isolate cDNAs that induce a loss of epithelial morphology, as indicative of a metastasis-inducing cDNA. Viruses transducing oncogenic (L61) Ras (Fig. 2C) were used as a positive control[10]. Screening and rescreening yielded a total of six confirmed cDNAs that induced a strong phenotype comparable to (L61) Ras (Fig. 2). Sequence analyses of the corresponding plasmids identified one hit as wild-type Ha-Ras (NM_005343) and a second hit as endothelin receptor B (XM_007109), a G protein–coupled receptor that has been implicated in metastasis formation of melanoma cells[11,12]. The remaining four hits encoded a C-terminal truncated form of cyclin-dependent kinase inhibitor (CDKI) p57Kip2 that had retained the kinase-inhibiting domain. Interestingly, a TAT-p27Kip1 fusion protein was previously found to induce scattering of HepG2 cells[13]. We

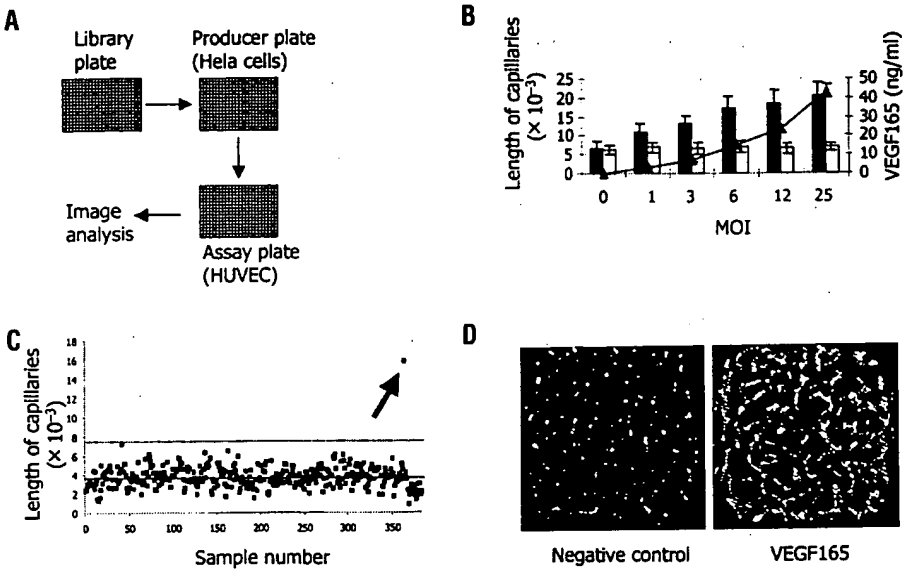

Figure 3. Capillary formation assay. (A) Schematic representation of the capillary formation assay. HeLa cells were infected with the placental adenoviral library. Conditioned medium was transferred after two days to HUVEC embedded in collagen. After 48 h, cells were stained with calcein-AM, and digital images of all wells were recorded. Image analysis was conducted using an algorithm that calculated the total length of the capillaries in a well. (B) To validate the capillary formation assay, HeLa cells were infected with an increasing MOI of Ad5/eGFP and Ad5/VEGF-165. The conditioned medium was tested in the capillary formation assay ($n = 28$) and analyzed in an ELISA detecting the VEGF-165 protein ($n = 4$). The total length of the capillaries per well induced by Ad5/eGFP and Ad5/VEGF-165 is represented by white and black bars, respectively. The corresponding VEGF-165 protein concentrations are depicted as black triangles. No VEGF-165 protein was detected in the conditioned medium of cells infected with eGFP adenovirus. (C) Graphic representation of a typical result of the capillary formation analysis. A baseline was set at the average capillary length of the total plate (solid line), and wells with a capillary length of more than the average + 3 s.d. (dotted line) were considered to be positive. (D) Photographs of wells of panel (C). The lefthand photograph shows a negative well, while the righthand photograph shows the positive well. Sequencing of the corresponding plasmid identified this hit as cDNA encoding VEGF-165.

are analyzing the downstream pathways required for scattering of MDCK cells by these CDKIs.

In a third screen, we attempted to identify novel modulators of angiogenesis. During angiogenesis, endothelial cells fuse to form tubes, a process that can be mimicked in an *in vitro* assay. The assay was set up as a two-step approach by infecting HeLa producer cells and transferring the conditioned medium after two days to primary human umbilical vein endothelial cells (HUVEC) (Fig. 3A). Viruses transducing vascular endothelial growth factor-165 (VEGF-165) were used as positive controls. The angiogenic properties of the conditioned medium were determined by measuring the length of capillaries formed by means of image analysis, using a modified algorithm (Fig. 3B, C). A total of three hits that scored above the average +3 s.d. were isolated after rescreening. Two of these encoded secreted proteins: (i) VEGF-165 that differed from the positive control in its 5′-untranslated region and (ii) CYR-61, a truncated cysteine-rich angiogenic inducer-61 variant that has been shown to promote tumor growth and vascularization[14]. The third hit encoded the interferon regulatory factor-I (IRF-I) transcription factor (GenBank NM_002198). IRF-I has not previously been associated with angiogenesis. Additional experiments are being done to understand the role(s) of this sequence in capillary formation.

In conclusion, we have screened part of an adenoviral PhenoSelect library in three different phenotypic assays. All three assays yielded genes known to be involved in the disease processes. In addition, we discovered new sequences and known genes that had not previously been related to these disease processes. Further validation work is in progress to characterize fully and validate these candidate genes.

As exemplified above, an important strength of the arrayed format lies in the wide range of assays that can be applied, such as those requiring morphological readouts and assays that have a relatively low signal-to-noise ratio. Designing an assay for a pooled library can be more difficult, in that it calls for a high level of sensitivity. Also, a particular disease-relevant phenotypic assay may require reconfiguration, which can be time-consuming. However, costs associated with screening of a pooled library can be lower than for arrayed libraries, and pooled libraries may also allow the use of fewer cells—an important consideration when using primary cells that are difficult to grow or obtain. A pooled library is usually faster and less costly to construct. Concerning library quality, pooled libraries can be much more complex and therefore cover very rare transcripts without arraying large numbers of clones. However, the construction of pooled libraries can lead to a bias and decrease in complexity. A defined arrayed library, consisting of discrete, nonredundant cDNAs, including very rare ones, will overcome most of the limitations of an undefined arrayed library. In summary, the adenoviral arrayed screening platform provides a tool to screen for disease-relevant gene functions, ultimately accelerating the development of novel drugs.

Experimental protocol

Construction of adenoviral library. The placental PhenoSelect cDNA library was constructed into the expression cassette of the pIPspAdApt6 adapter plasmid[4], which contains part of the adenoviral genome. Individual bacterial clones of the primary library were grown overnight in 96-well plates in standard Luria–Bertani (LB) medium. Bacteria were precipitated and processed by a modified alkaline lysis procedure[15] using an integrated liquid-handling system. The resulting plasmids were quantified using SYBR Green (Molecular Probes Europe, Leiden, The Netherlands), digested with PI-PspI to release the adenoviral sequences, and co-transfected into the PER.C6/E2A adenoviral packaging cells together with the helper cosmid DNA containing the remaining part of the adenoviral genome. Transfections were carried out in 96-well plates on a Jobi-Well (Jenoptik, Jena, Germany) using a master mix of helper DNA and lipofectamine (Invitrogen, Carlsbad, CA) in DMEM. Three weeks after transfection, crude lysates were obtained by freeze-thawing and used to propagate the viruses. The average titer of the library was determined by RT-PCR[5].

Osteoblast differentiation. Human MSC were seeded in 60 µl of α-MEM (Invitrogen) containing 10% (vol/vol) FBS at 1,000 cells/well in black 384-well plates with clear bottoms. To optimize transduction efficiencies of Ad5 viruses, we infected the cells with a capsid-modified virus transducing the hCAR[6]. Ad5-hCAR virus was added to each well 24 h after plating at an MOI of 100, followed by control viruses or viruses from the PhenoSelect library at an average MOI of 5,000. Following incubation for six days at 37°C, 10 µl of a 4-methylumbelliferyl heptaphosphate

(MUP) solution (Sigma-Aldrich, St. Louis, MO) was added to each well. Plates were incubated for 15 min at 37°C and measured on a Fluostar fluorescence reader (BMG, Offenburg, Germany). For each plate, an average fluorescence value and a standard deviation were calculated; any well that scored more than the average plus 3 s.d. was scored as a hit.

To discriminate between bone-specific alkaline phosphatase and other alkaline phosphatases, total RNA from MSC was extracted seven days post infection using Trizol (Invitrogen). Primers specific for bone-specific alkaline phosphatase for SYBRGreen real-time PCR (Applied Biosystems, Foster City, CA) were as follows: forward, 5′-CATGCTGAGTGACACAGACAAGAAG-3′; reverse, 5′- TGGTAGTTGTTGTGAGCATAGTCCA-3′. Data were normalized for GAPDH levels, using GAPDH-specific primers: forward, 5′-GAAGGTGAAGGTCGGAGTC-3′; reverse, 5′-GAAGATGGTGATGGGATTTC-3′.

Scatter assay. MDCK-2 cells were cultured in DMEM (Invitrogen) containing 10% (vol/vol) heat-inactivated FBS. The cells were seeded in 96-well plates at a density of 1.5×10^3 cells/well. Cells were infected 20 h after seeding at an average MOI of 2,500. The supernatant was removed 48 h post infection and 50 µl of 0.5 µM calcein-AM (Molecular Probes Europe) in PBS were added. The plates were incubated in the dark at room temperature for 30 min. Readout was conducted using a fluorescence microscope, and all wells were visually inspected for the presence of cells that grow in islands (i.e., have remained epithelial) versus cells that grow individually (i.e., have scattered).

Capillary formation assay. HeLa cells were cultured in DMEM containing 10% FBS (vol/vol) and were seeded in a 384-well plate at a cell density of 5,000 cells/well in SFM medium (Invitrogen). They were infected at an average MOI of 200 and incubated for 48 h. HUVEC were cultured in EBM2-supplemented medium (Clonetics–Biowhittaker, Verviers, Belgium). They were made quiescent 48 h before use, embedded in collagen type I (Sigma-Aldrich) as described[16], and seeded in a 384-well plate. Cells were stained with calcein-AM 48 h after transfer of the conditioned medium from the HeLa cells to the HUVEC, and images were recorded. Image analysis was done using an algorithm consisting of adaptative thresholding for background subtraction, followed by a skeletonization procedure to determine the length of the capillaries. Concentration of VEGF-165 protein was determined by ELISA (R&D, Minneapolis, MN).

Note: Supplementary information is available on the Nature Biotechnology website.

Acknowledgments

We acknowledge the gift of mesenchymal stem cells by IsoTis (Bilthoven, The Netherlands). We thank John Collard for providing the MDCK cells. This work was supported in part by an IWT grant from the Flemish government.

Competing interests statement

The authors declare competing financial interests: see the Nature Biotechnology website (http://biotech.nature.com) for details.

Received 14 March 2002; accepted 15 August 2002

1. Wright, F.A. *et al.* A draft annotation and overview of the human genome. *Genome Biol.* **2**, 0025.1–0025.18 (2001).
2. Hogenesch, J.B. *et al.* A comparison of the Celera and Ensembl predicted gene sets reveals little overlap in novel genes. *Cell* **106**, 413–415 (2001).
3. Fallaux, F.J. *et al.* Means and methods for nucleic acid delivery vehicle design and nucleic acid transfer. US 6,395,519 (2002).
4. Schouten, G., Vogels, R., Bout, A. & Van Es, H. High-throughput screening of gene function using libraries for functional genomics applications. US 6,430,595 (2002).
5. Ma, L. *et al.* Rapid determination of adenoviral vector titres by quantitative real-time PCR. *J. Virol. Methods* **93**, 181–188 (2001).
6. Bergelson, J.M. *et al.* Isolation of a common receptor for Coxsackie B viruses and adenoviruses 2 and 5. *Science* **275**, 1320–1323 (1997).
7. Rodan, G.A. & Harada, S. The missing bone. *Cell* **89**, 677–680 (1997).
8. Service, R.F. Tissue engineers build new bone. *Science* **289**, 1498–1500 (2000).
9. Sabatakos, G. *et al.* Overexpression of DeltaFosB transcription factor(s) increases bone formation and inhibits adipogenesis. *Nat. Med.* **6**, 985–990 (2000).
10. Behrens, J., Mareel, M.M., Van Roy, F.M. & Birchmeier, W. Dissecting tumor cell invasion: epithelial cells acquire invasive properties after the loss of uvomorulin-mediated cell–cell adhesion. *J. Cell Biol.* **108**, 2435–2447 (1989).
11. Demunter, A., De Wolf-Peeters, C., Degreef, H., Stas, M. & van den Oord, J.J. Expression of the endothelin-B receptor in pigment cell lesions of the skin. Evidence for its role as tumor progression marker in malignant melanoma. *Virchows Arch.* **438**, 485–491 (2001).
12. Voumakis, J.N., Finkielsztein, S. & Pariser, E.R. Methods and compositions for treatment of cell proliferative disorders. Patent Application US 6,063,911 (2000).
13. Nahagara, H. *et al.* Transduction of full-length TAT fusion proteins into mammalian cells: TAT-p27Kip1 induces cell migration. *Nat. Med.* **4**, 1449–1452 (1998).
14. Babic, A.M., Kireeva, M.L., Kolesnikova, T.V. & Lau, L.F. CYR61, a product of a growth factor-inducible immediate early gene, promotes angiogenesis and tumor growth. *Proc. Natl. Acad. Sci. USA* **95**, 6355–6360 (1998).
15. Sambrook, J. & Russel, D.W. *Molecular Cloning: A Laboratory Manual.* (Cold Spring Harbor Laboratory Press, Cold Spring Harbor, NY, 2001).
16. Montesano, R. & Orci, L. Tumor-promoting phorbol esters induce angiogenesis *in vitro*. *Cell* **42**, 469–477 (1985).